

Supplementary Information

S-dimethylarsino-glutathione (darinaparsin®) targets histone H3.3, leading to TRAIL-induced apoptosis in leukemia cells

Xiaohan Xu,^{a†} Haibo Wang,^{a†} Hongyan Li,^a Xuqiao Hu,^a Yu Zhang,^b Xinyuan Guan,^b
Patrick H Toy,^a Hongzhe Sun^{*a}

^a Department of Chemistry, The University of Hong Kong, Pokfulam Road, Hong Kong,
P. R. China

^b Department of Clinical Oncology, Li Ka Shing Faculty of Medicine, The University of
Hong Kong, Sassoon Road, Hong Kong, P. R. China

† These authors contributed equally to this work

* Corresponding author: Prof. Hongzhe Sun

E-mail: hsun@hku.hk

Table of Contents

Table of Contents	2
Experimental Procedures	4
Materials and Reagents	4
Apparatus	4
Cell Culture and Fractionation	4
Identification of Arsenic Binding Protein in Cell Nuclei Fractions by GE-ICP-MS	5
Arsenic Content Determination of histone H3.3	6
MALDI-TOF-MS	6
Cellular Thermal Shift Assay (CETSA)	6
Ellman's Assay	7
Modified SDS-PAGE	7
Circular Dichroism Studies of Reconstituted Core Histones	7
Thermal Denaturation of Reconstituted Nucleosomes	8
Real-Time PCR	8
Gene Knockdown	9
Apoptosis Detection by Flow Cytometry	9
Supplementary Figures and Tables	10
Fig. S1. Cell viability of NB4 and HL60 cells under different concentrations of ZIO-101 and ATO.	10
Fig. S2. GE-ICP-MS analyses for the nuclei of NB4 cells treated with magnetic beads..	11
Fig. S3. GE-ICP-MS analyses for the nuclei of PBMC cells treated with ZIO-101.	12
Fig. S4. <i>In vitro</i> binding of ZIO-101 to histone H3.3 detected by GE-ICP-MS.	13
Fig. S5. The binding stoichiometry of ZIO-101 to histone H3.3 measured by ICP-MS...14	
Fig. S6. Binding ratio between ATO and histone H3.3 analyzed by MALDI-TOF-MS. .15	
Fig. S7. Time-dependent ⁷⁵ As GE-ICP-MS profiles of nuclear protein from NB4 and HL60 cells after treatment with ZIO-101.	16
Fig. S8. Cellular thermal shift assay (CETSA) of histone H3.3 in NB4 cells treated with ATO.	17
Fig. S9. Free cysteine detection.	18
Fig. S10. Disruption of histone H3.3 dimerization by the binding of ZIO-101.	19
Fig. S11. Circular dichroism study regarding the effects of ZIO-101 binding to histone H3.3 on nucleosome structure.	20
Fig. S12. Representative thermal denaturation (<i>T_m</i>) curves of nucleosomes formed by DNA and histones with or without ZIO-101 treatment.	21
Fig. S13. PPI (protein-protein interactions) of genes involved in transcriptional misregulation in cancers.	22
Fig. S14. A heat map showing expression profiles of genes involved in transcriptional misregulation in cancers.	23
Fig. S15. Flow cytometry plots for detecting apoptosis of NB4 cells after transfection study.	24
Table S1. Properties of Iodine-labelled standard proteins	25
Table S2. Peptide mass fingerprints of histone H3.3	26

Table S3. Information of the selected genes involved in ‘transcriptional misregulation in cancers’	27
Table S4. Primer sequences of the selected genes studied in RT-PCR (5’–3’).....	29
Table S5. Fold changes of apoptosis related genes in NB4 cells treated with ZIO-101. ...	32
Supplementary Text	33
References	34

Experimental Procedures

Materials and Reagents

NB4 cells and HL60 cells were provided by Dr. Eric Tse (Department of Medicine, the University of Hong Kong). Arsenic trioxide (purity, $\geq 99.0\%$), Cell Proliferation Kit II (XTT), Multielement standard solution (51844) for ICP-MS detection of ^{75}As and Amicon Ultra 0.5 mL centrifugal filters (3kDa MWCO, Millipore) were purchased from Sigma-Aldrich (St. Louis, MO, USA). ZIO-101 was bought from TRC Canada. RPMI1640 medium, fetal bovine serum (FBS) and penicillin-streptomycin solution were purchased from Life Technologies. Anti-histone H3.3 antibody and anti-rabbit IgG antibody were purchased from Abcam and Gene Company Limited (HK), respectively. Ultrapure Millipore (Mini-Q) water (18.2 M Ω) was used throughout the experiments.

Apparatus

The GE-ICP-MS system consisting a column-type gel electrophoresis for protein separation, ICP-MS (Agilent 7700x, Agilent Technologies, CA, USA) for elemental-specific analysis, and a peristaltic pump for transferring the eluents from the GE system to ICP-MS and the sample collection tubes was used in this work to identify arsenic-binding protein in cell nuclei fractions¹.

Cell Culture and Fractionation

NB4 and HL60 cells were cultured in RPMI1640 medium supplemented with 100 $\mu\text{g}/\text{mL}$ penicillin, 100 $\mu\text{g}/\text{mL}$ streptomycin and 10% heat-inactive FBS. Then, the cells were incubated in a 5% CO_2 humidified incubator at 37°C and typically passaged with sub-cultivation ratio of 1:4 every two days. Cell viability of NB4 and HL60 cells were tested separately using 96 well plates with a gradient of ATO or ZIO-101 (0, 1, 5, 10, 50, 100 μM) for 7 hrs by an XTT cell proliferation assay. 200 mL of NB4/HL60 cells were treated with ATO/ZIO-101 at the IC_{50} concentration value for 7 hrs. Then the cells were harvested and washed with ice-cold phosphate-buffered saline (PBS of 1.9 mM NaH_2PO_4 , 8.1 mM Na_2HPO_4 , and 154 mM NaCl at pH 7.4) for three times. The cell pellets were re-suspended in 5 packed cell pellet volumes of hypotonic buffer A (10 mM HEPES, 10 mM KCl , 1.5 mM MgCl_2 , pH 7.5) in the presence of a protease inhibitor cocktail (PIC) and placed on ice for 10 min. Subsequently, the cells were lysed by 10 stokes of a Kontes all-glass Dounce homogenizer that was washed with ultrapure water and then rinsed with buffer A. The homogenate was checked microscopically for cell lysis and centrifuged for 10 min at 3000g to pellet the nuclei. The nuclei pellets were washed with buffer A for three times and then buffer B (20 mM HEPES,

420 mM NaCl, 1.5 mM MgCl₂, 25% glycerol, pH 7.5) containing PIC were added and the nuclei pellets were sonicated for 2 min. The supernatant containing nuclear proteins was collected by spinning at 20 000g for 30 min at 4°C. Protein concentrations were detected by bicinchoninic acid (BCA) assays (Novagen) and samples were snap frozen for further use².

Identification of Arsenic Binding Protein in Cell Nuclei Fractions by GE-ICP-MS

Generally, a reverse double layer SDS gel (15% → 13% with volumes of 140 µL and 120 µL, respectively) was used for separating NB4/HL60 nuclear proteins in GE-ICP-MS. A 4% SDS gel with the volume of 200 µL was casted on top as the stacking gel.

Approximately 50 µg samples were mixed with 1x loading buffer (0.5 M Tris-HCl buffer, pH 6.8, 25% glycerol (v/v)) and loaded onto the stacking gel. Gel electrophoresis was conducted under a consecutive two-step voltage program (60 min at 200 V and 600 V till the end) and the arsenic-binding protein was eluted in the last step. ICP-MS was run in the time-resolved analysis (TRA) mode (RF Power 1550 W, Sampling depth 7 mm) for monitoring arsenic signals associated with eluted protein fractions. A T-connection tubing was applied to split the elute from the gel electrophoresis separation, transferring half of the solution to ICP-MS and the other half to the sample collection tubes for protein identification. One-dimensional SDS-PAGE gels were subsequently used to separate the collected fractions, which also helped to concentrate the arsenic-binding proteins.

The iodine-labeled proteins³ (Lysozyme, Carbonic anhydrase and Ovalbumin from GE Healthcare) were utilized to be protein markers during the GE-ICP-MS analyses. 1D SDS-PAGE gels with 15% gel were used to separate protein fractions collected in GE-ICP-MS. Protein samples with the same volume were analyzed using SDS-PAGE and then the gels were further silver-stained.

The proteins in gel pieces were extracted and identified through peptide mass fingerprinting according to the standard protocol. In detail, the proteins in gel pieces were extracted twice using 5% formic acid (FA)/50% acetonitrile (ACN) and then extracted once with 100% ACN. After purification by Ziptip (Millipore), the desalted peptides were mixed in a 1:1 ratio with 10 mg/ml α -cyano-4-hydroxycinnamic acid matrix (Fluka) dissolved in 0.1% FA/50% ACN.

The samples were injected via a nanospray chamber equipped with a gold coated nanospray tip (New Objective). Protein identification and characterization were performed by using the 4800 MALDI TOF/TOF Analyser (ABSciex) which was equipped with a Nd:YAG laser that operates at 355 nm to ionize the samples. All mass spectra were acquired in positive ion reflector mode using the 4000 series explorer version 3.5.28193 software (ABSciex). Each sample was analyzed with

MALDI-TOF MS to create the peptide mass fingerprinting (PMF) data (scanning range of 900-4000 m/z). The peak detection criteria for MS/MS used were an S/N of 5 and a local noise window width of 250 (m/z) and a minimum full-width half maximum (bins) of 2.9. The combined PMF and MS/MS search was then performed using GPS Explorer algorithm version 3.6 (ABSciex) against the non-redundant NCBI database using the in-house MASCOT search engine version 2.2¹. The criteria for protein identification were based on the probability score of each search result. Significant matches had scores greater than the minimum threshold set by MASCOT ($P < 0.05$).

Arsenic Content Determination of histone H3.3

The ⁷⁵As contents of histone H3.3 were determined by an Agilent 7700x inductively coupled plasma mass spectrometry (ICP-MS) spectrometer (Agilent Technologies, CA, USA) in a time-resolved analysis mode. The running conditions of ICP-MS were listed as follows: nebulizer (glass concentric), RF power (1550 W), Sampling depth (7.0 mm), Carrier gas (0.8 L/min), measurement duration (60 s). Each sample was quantified in triplicate and the average value was used. Histone H3.3 in Tris-HNO₃ buffer was incubated with ZIO-101 at the IC₅₀ value for 7 hrs at 4 °C, and then excess amounts of ZIO-101 were removed by ultrafiltration using Amicon Ultra 0.5 mL centrifugal filters (3 kDa MWCO). The protein concentration was measured by a BCA assay, and the bound arsenic was determined by ICP-MS. The standard curve of arsenic with concentration ranging from 1 ppb to 100 ppb was prepared from a multielement standard solution (90243, Sigma-Aldrich) for ICP-MS. Arsenic contents in proteins were calculated according to the standard curve.

MALDI-TOF-MS

MALDI-TOF-MS was performed using the 4800 MALDI-TOF/TOF-MS (AB Sciex). 15 μM histone H3.3 (Sigma, H2542) in 20 mM Tris-HNO₃ buffer (pH 7.4) was incubated with ATO or ZIO-101, respectively at room temperature for 2hrs at varying molar ratios (histone H3.3: Arsenicals=1:0, 1:1, 1:2). Subsequently, 1 μL aliquot of each sample was mixed with 1 μL of 10 mg/mL Sinapinic acid matrix (Sigma) that had been dissolved in 0.1% TFA/50%ACN and the mixture was spotted onto the plate and dried before analysis. All mass spectra were acquired using the 4000 Series Explorer software (AB Sciex) under the positive ion linear mode with a laser intensity of 6000 and a delay time of 610 ns. Before the detection, the MS was calibrated using the CalMix#3 (AB Sciex; thionredoxin 11674Da and apomyoglobin 16952Da).

Cellular Thermal Shift Assay (CETSA)

100 mL of NB4 cells (1.5 to 2×10^6 cells/mL) were treated with ATO/ZIO-101 under IC_{50} values for 7 hrs, and then harvested by centrifugation at 1000 g for 10 min at $4^{\circ}C$. Afterwards, the cells were re-suspended in 10 mL ice-cold PBS and washed three times under identical conditions. The cell pellets were collected and re-suspended in 1.5 mL ice-cold PBS. 100 μ L of the cell suspension was transferred into 0.2 mL PCR tubes, and each tube was heated in parallel in a PCR machine for 6 min to the respective temperature ($50^{\circ}C$ to $86^{\circ}C$). The tubes were then incubated for 6 min at room temperature. Subsequently, samples were frozen in liquid nitrogen for 3 min and then thawed in a $25^{\circ}C$ water bath for 3 min. This freeze-thaw cycle was repeated five times. The entire content was centrifuged at 14,000 rpm for 20 min at $4^{\circ}C$. After centrifugation, 70 μ L of each supernatant was transferred into new tubes. The protein concentration of the $50^{\circ}C$ sample was determined and used to normalize loading volume of SDS gels. Proteins in the supernatant were denatured using the SDS sample buffer, partially separated by means of SDS gel electrophoresis, and subjected to a western blot assay using H3.3 antibodies.

Ellman's assay

According to previous report⁴, 100 μ M histone H3.3 (Sigma, H2542) was incubated with different molar equivalents of ZIO-101 at room temperature for 30 mins. Then excess amounts of 5,5'-Dithiobis-(2-nitrobenzoic acid) (DTNB) were added into samples to reach a final concentration of 300 μ M and further incubated for 20 mins. A Cary 50 UV-Vis spectrometer was used to record UV absorbance at 412 nm⁵ for each sample and the data was plotted against the ZIO-101/protein ratio. The Ellman's assay was carried out in phosphate buffer (20 mM NaPO₄, 0.3 M NaCl, pH=7.0).

Modified SDS-PAGE

Modified SDS-PAGE was carried out in a mini vertical gel system. After dialyzed in different situations, histone H3.3 was diluted in loading buffer (0.2 M Tris-HCl buffer, pH 6.8, 20% glycerol (v/v)) and separated by 13% (m/v) acrylamide separating gel and 4% (m/v) stacking gel in Tris-glycine running buffer (25 mM Tris, 192 mM glycine, pH 8.3). The modified SDS-PAGE condition was 90 V for 15 min and 150 V for 1 h in an ice-water chamber. Then the gel was stained with Coomassie brilliant blue (CBB) R-250 to analyze the molecular weight of protein bands.

Circular Dichroism Studies of Reconstituted Core Histones

A Jasco spectropolarimeter (model J-720) was utilized to perform circular dichroism (CD) measurements under a constant temperature of $25^{\circ}C$. Recombinant H3.3 core histone proteins

(SKU: 16-8012, EpiCypher, USA) were dissolved in 10 mM potassium phosphate, 100 mM KCl buffer (pH 7.4) to make a final concentration of 10 μ M, ZIO-101/ATO was prepared to a final concentration of 40 μ M. Control or arsenical-treated samples were placed in a 0.1 cm path-length quartz cuvette and the spectra were recorded from 190 to 280 nm and repeated three times. The scan speed and response time of CD spectra were settled to be 20 nm/min and 0.25s, respectively. Experiments were repeated three times to confirm repeatability of the results. CDNN7.0 software package was used to conduct the quantitative estimation of the contents of secondary structures.

Thermal Denaturation of Reconstituted Nucleosomes

Recombinant H3.3 core histone proteins (SKU: 16-8012, EpiCypher, USA) and human DNA (Sigma) were utilized for the reconstitution of nucleosomes. Histones were treated with 1 mM ZIO-101 and then ultra-filtered using Amicon Ultra 0.5 mL centrifugal filters (3kDa MWCO). Subsequently, the reconstitution experiments were carried out according to previously reported protocol⁵ by mixing histones and DNA at the ratio of 1:1. Thermal denaturation studies were conducted on a Varian Cary 50 spectrophotometer equipped with a single cell Peltier Accessory based on the reported procedures⁶. The melting point was calculated using the Savitsky-Golay algorithm⁷.

Real-Time PCR

Real-time PCR to measure gene expression levels in NB4 cells was performed under the instruction of previous literature⁸. NB4 cells were seeded in P100 Petri dishes at 2×10^6 and then cultured for 12 hrs at 37 °C in a humidified incubator containing 5% CO₂. After that, cells were treated for 0, 6, 12 and 24 hrs with 5 μ M ZIO-101 and six biological replicates were prepared for each ZIO-101 treatment group with three of them being combined for total RNA extraction. Total RNA was extracted using RNA Extraction Kit (Takara, Japan) according to manufacturer's instructions with slight modifications and collected in 100 μ L RNase-free water and stored at -80 °C. A NanoDrop 1000 spectrophotometer was used to check RNA quality and to estimate RNA concentration. Reverse transcription was performed using PrimeScript™ RT Master Mix (Perfect Real Time, Takara, Japan) and obtained cDNA was used for Real-Time PCR. Real-Time PCR was conducted using TB Green™ Premix Ex Taq™ (Takara, Japan) and specific primers (sequences are listed in Table S3) on StepOnePlus Real-Time PCR system (Applied Biosystems, USA). cDNA for each sample and the non-template control were used in the detection of each target gene. The transcription level of target genes was quantified using $\Delta\Delta$ Ct method^{9, 10}. GAPDH was used as an internal control and expression of target genes was calculated relative to GAPDH expression.

Gene Knockdown

The histone H3.3-specific siRNA and negative control siRNA were synthesized and purchased from Thermo Scientific. NB4 cells were plated in 12-well culture plates at the density of 2×10^5 in 1 mL RPMI1640 medium without antibiotics one day before transfection and then transfected with siRNA using Lipofectamine™ 2000 reagent (Invitrogen). For each transfection sample, 20 pmol siRNA oligomer was diluted in 100 μ L Opti-MEMI reduced serum medium (Invitrogen). This mixture was mixed with 2 μ L Lipofectamine™ 2000 diluted in 100 μ L Opti-MEMI medium and then the mixture was incubated at room temperature for 20 mins. Subsequently, the siRNA-Lipofectamine™ 2000 complexes were gently added into cells. PRMI1640 medium containing antibiotics were added after NB4 cells were transfected for 6 hrs. The cells were harvested and lysed after 24 hrs and histone H3.3 was quantified using Western blotting assay¹¹.

Apoptosis Detection by Flow Cytometry

ZIO-101 induced apoptosis in NB4 cells before and after histone H3.3 silencing were detected using the Annexin V-FITC apoptosis detection kit (Thermo Scientific). NB4 cells were plated in 6-well culture plates at the density of 1×10^6 in 2 mL RPMI 1640 medium. After silenced using negative control siRNA or histone H3.3-specific siRNA, NB4 cells were treated with 5 μ M ZIO-101 for 12 hrs. Then NB4 cells were harvested and washed 3 times using could 1xPBS. Samples were stained by Annexin V-FITC and propidium iodide (PI) according to the kit's protocol. After incubated in the dark for 15 mins at room temperature, the samples were analyzed by flow cytometry with FITC filters and PI filters. Data were processed using Flowjo software.

Supplementary Figures and Tables

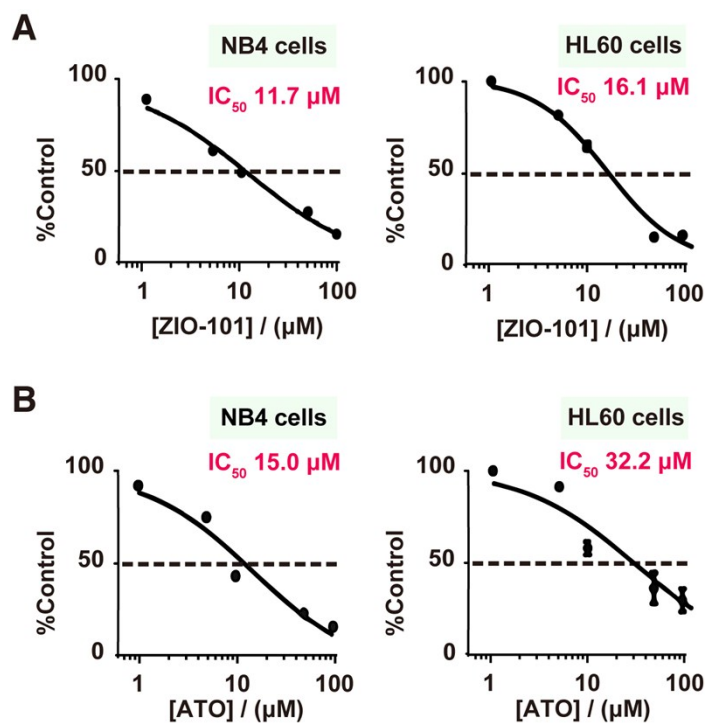


Fig. S1. Cell viability of NB4 and HL60 cells under different concentrations of ZIO-101 and ATO. (A) ZIO-101 treatment. (B) ATO treatment. The curves were plotted according to XTT cell proliferation assay.

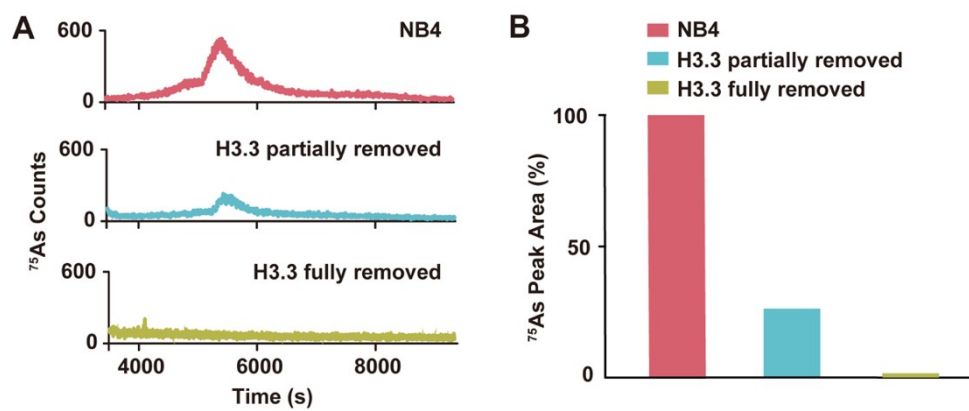


Fig. S2. GE-ICP-MS analyses for the nuclei of NB4 cells treated with magnetic beads. (A) GE-ICP-MS profiles of ^{75}As . (B) Peak area of ^{75}As .

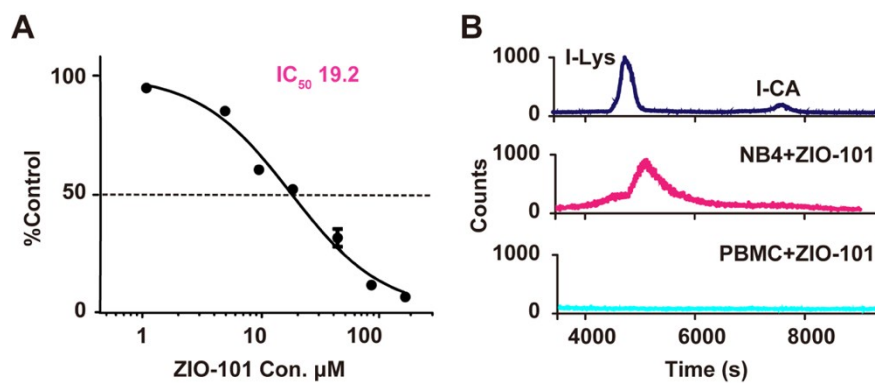


Fig. S3. GE-ICP-MS analyses for the nuclei of PBMC cells treated with ZIO-101. **(A)** Cell viability for PBMC cells under different concentrations of ZIO-101. The figures were plotted according to XTT cell proliferation assay. **(B)** GE-ICP-MS profiles of I-labeled standard proteins, arsenic-binding proteins in nuclei of ZIO-101 treated NB4 cells and PBMC cells.

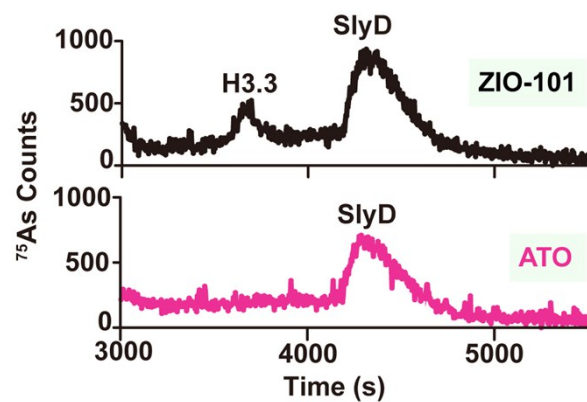


Fig. S4. *In vitro* binding of ZIO-101 to histone H3.3 detected by GE-ICP-MS. GE-ICP-MS profiles of ⁷⁵As in histone H3.3 and SlyD incubated with ZIO-101 (up) or ATO (down) for 12 hrs.

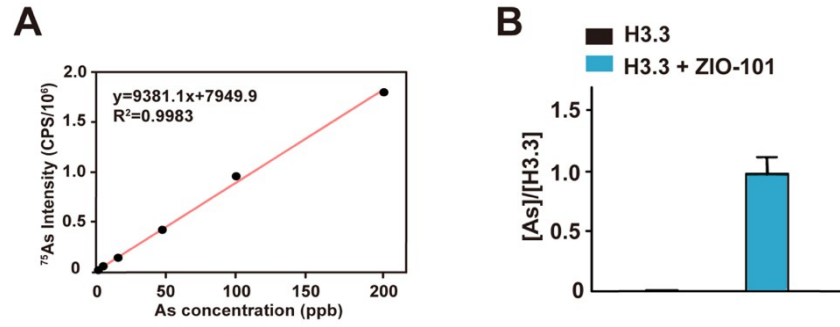


Fig. S5. The binding stoichiometry of ZIO-101 to histone H3.3 measured by ICP-MS. (A) ^{75}As calibration curve using standard arsenic solution by ICP-MS. (B) ^{75}As -binding capacity of histone H3.3. The arsenic contents were detected by ICP-MS and protein concentrations were measured by BCA assay.

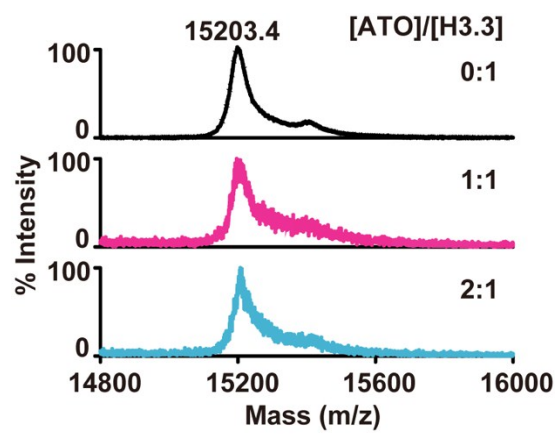


Fig. S6. Binding ratio between ATO and histone H3.3 analyzed by MALDI-TOF-MS.

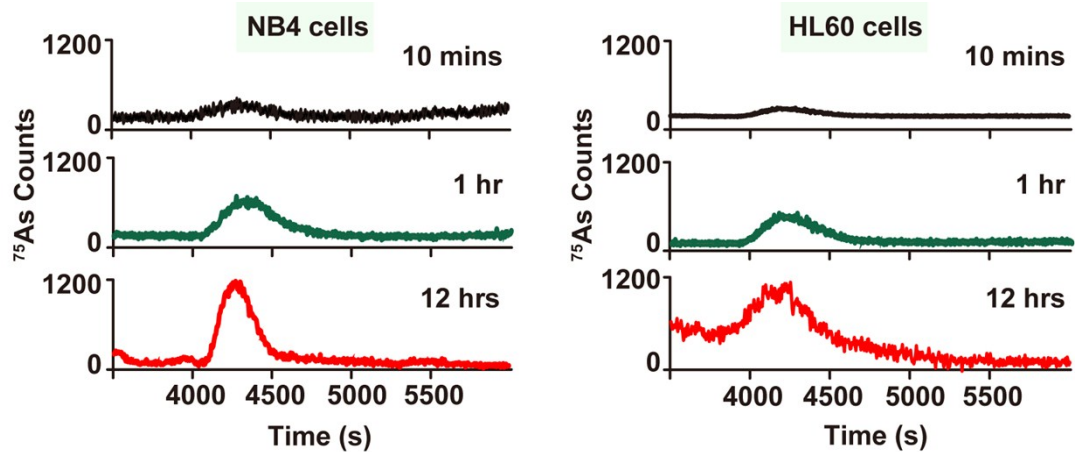


Fig. S7. Time-dependent ^{75}As GE-ICP-MS profiles of nuclear protein from NB4 and HL60 cells after treatment with ZIO-101.

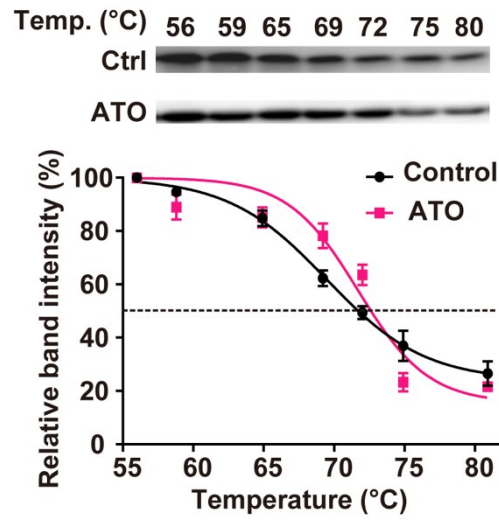


Fig. S8. Cellular thermal shift assay (CETSA) of histone H3.3 in NB4 cells treated with ATO. Each point plotted represents the mean of three replicates for each temperature; error bars denote \pm SD.

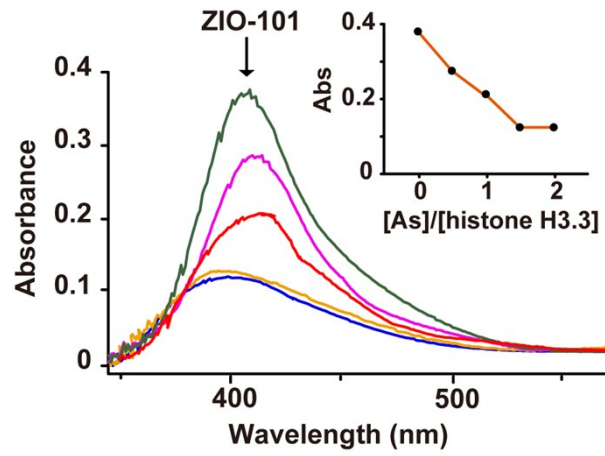


Fig. S9. Free cysteine detection. Changes of free cysteine contents before/after ZIO-101 incubation of histone H3.3 were monitored by Ellman's assay.

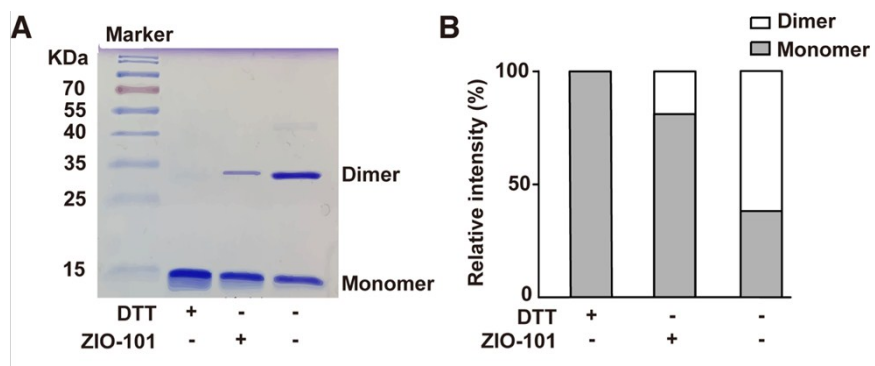


Fig. S10. Disruption of histone H3.3 dimerization by the binding of ZIO-101. (A) Modified SDS-PAGE of histone H3.3 after dialysis in buffer containing ZIO-101 or DTT. (B) Relative band intensities of monomers and dimers in histone H3.3 under different dialysis conditions.

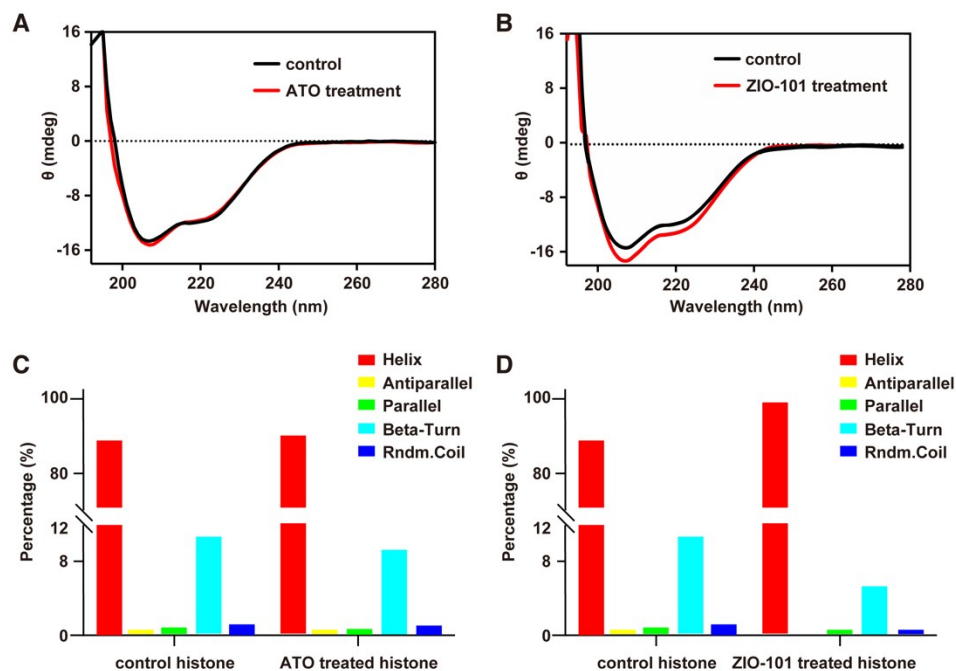


Fig. S11. Circular dichroism study regarding the effects of ZIO-101 binding to histone H3.3 on nucleosome structure. (A)(B) Representative Circular Dichroism curves for control and ATO/ZIO-101 treated reconstituted nucleosomes. (C)(D) Quantitative estimation of the contents of secondary structures.

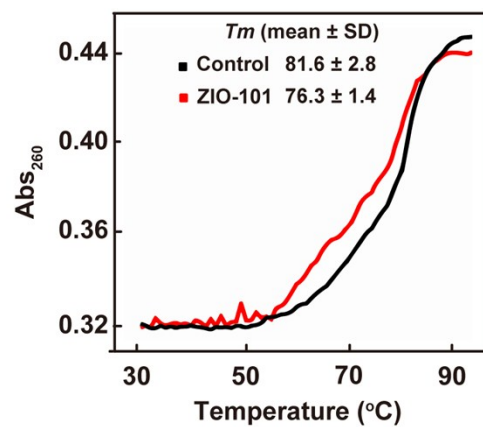


Fig. S12. Representative thermal denaturation (T_m) curves of nucleosomes formed by DNA and histones with or without ZIO-101 treatment. *Inset:* T_m values obtained from three independent experiments (mean \pm SD).

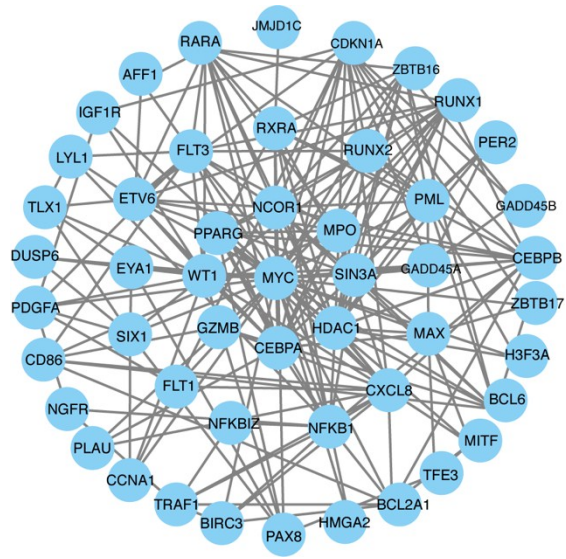


Fig. S13. PPI (protein-protein interactions) of genes involved in transcriptional misregulation in cancers. The functional category is analyzed by STRING and viewed by Cytoscape.

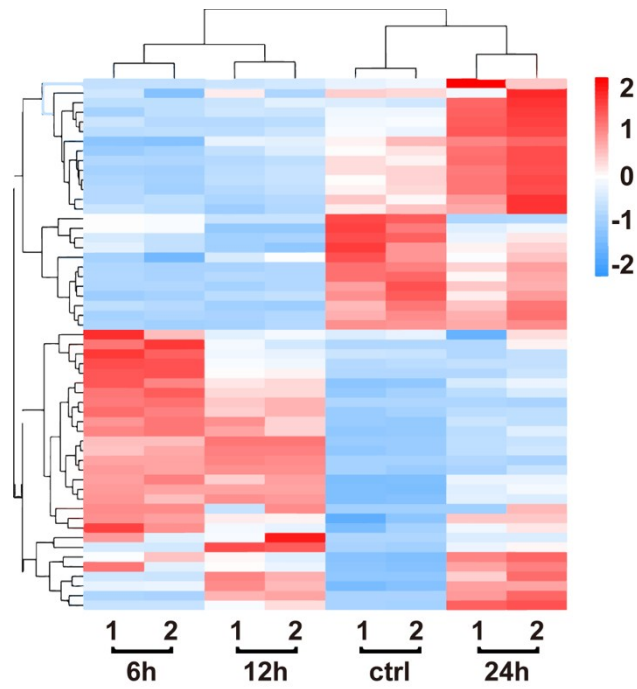


Fig. S14. A heat map showing expression profiles of genes involved in transcriptional misregulation in cancers.

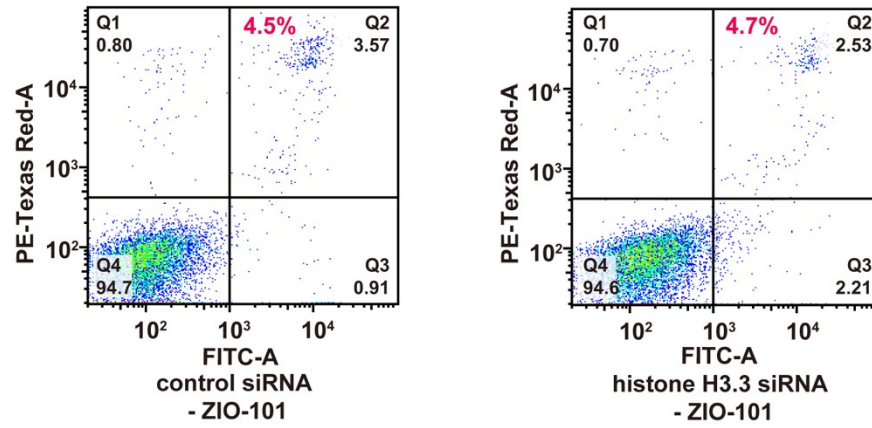


Fig. S15. Flow cytometry plots for detecting apoptosis of NB4 cells after transfection study.
(A) NB4 cells were transfected with negative control siRNA. **(B)** NB4 cells were transfected with histone H3.3 siRNA.

Table S1. Properties of Iodine-labelled standard proteins

Proteins	pI	Theoretical molecular mass (kDa)	Calibrated molecular mass (kDa)
Lysozyme	10.5	14.4	14.9
Carbonic anhydrase	6.2	29.0	30.1
Ovalbumin	4.7	44.0	45.3

Table S2. Peptide mass fingerprints of histone H3.3

Protein Name	Accession No.	Protein Score	Protein Score C.I.%	Molecular Mass
histone H3.3 [Homo sapiens]	AAH81561.1	128	100	15332.5
Peptide Information				
Calc. Mass	Obs. Mass	Peptide Sequence	Modification	Ion Score
990.5578	990.6066	QTALKSTGGK		
1028.6364	1028.6772	LPFQRLVR		
1032.595	1032.6504	YRPGTVALR		
1032.595	1032.6504	YRPGTVALR		19
1218.6841	1218.746	LVREIAQDFK		
1250.7103	1250.7753	YQKSTELLIR		
1335.6903	1335.7584	EIAQDFKTDLR		
1335.6903	1335.7584	EIAQDFKTDLR		62
1430.8226	1430.8873	YRPGTVALREIR		

Table S3. Information of the selected genes involved in ‘transcriptional misregulation in cancers’.

Gene Symbol	Gene Description
CXCL8	Interleukin-8
BCL2A1	Bcl-2-related protein A1
GADD45A	Growth arrest and DNA damage-inducible protein GADD45 alpha
PLAU	Urokinase-type plasminogen activator
CEBPA	CCAAT/enhancer-binding protein alpha
TRAF1	TNF receptor-associated factor 1
WT1	Wilms tumor protein
NFKBIZ	NF-kappa-B inhibitor zeta
FLT1	Vascular endothelial growth factor receptor 1
TFE3	Transcription factor E3
BCL6	B-cell lymphoma 6 protein
PDGFA	Platelet-derived growth factor subunit A
ZBTB16	Zinc finger and BTB domain-containing protein 16
H3F3A	Histone H3.3
HDAC1	Histone deacetylase 1
PPARG	Peroxisome proliferator-activated receptor gamma
BIRC3	Baculoviral IAP repeat-containing protein 3
GADD45B	Growth arrest and DNA damage-inducible protein GADD45 beta
SIN3A	Paired amphipathic helix protein Sin3a
CEBPB	CCAAT/enhancer-binding protein beta
RXRA	Retinoic acid receptor RXR-alpha
ZBTB17	Zinc finger and BTB domain-containing protein 17
IGF1R	Insulin-like growth factor 1 receptor
LYL1	Protein lyl-1
DUSP6	Dual specificity protein phosphatase 6
JMJD1C	Probable JmjC domain-containing histone demethylation protein 2C

Gene Symbol	Gene Description
MPO	Myeloperoxidase
NFKB1	Nuclear factor NF-kappa-B p105 subunit
CDKN1A	Cyclin-dependent kinase inhibitor 1
NCOR1	Nuclear receptor corepressor 1
PER2	Period circadian protein homolog 2
HMGA2	High mobility group protein HMGI-C
PML	Protein PML
ETV6	Transcription factor ETV6
RUNX1	Runt-related transcription factor 1
MYC	Myc proto-oncogene protein
FUT8	Alpha-(1,6)-fucosyltransferase
PAX8	Paired box protein Pax-8
MAX	Protein max
RUNX2	Runt-related transcription factor 2
RARA	Retinoic acid receptor alpha
GZMB	Granzyme B
CD86	T-lymphocyte activation antigen CD86
AFF1	AF4/FMR2 family member 1
SLC45A3	Solute carrier family 45 member 3
CCNA1	Cyclin-A1
NGFR	Tumor necrosis factor receptor superfamily member 16
FLT3	Receptor-type tyrosine-protein kinase FLT3
BAK1	Bcl-2 homologous antagonist/killer
ITGB7	Integrin beta-7
TLX1	T-cell leukemia homeobox protein 1
SIX1	Homeobox protein SIX1
EYA1	Eyes absent homolog 1
ETV7	Transcription factor ETV7

Table S4. Primer sequences of the selected genes studied in RT-PCR (5'–3').

	Forward Primers	Reverse Primers
IRF1	CTC TCA CCA AGA ACC AGA GAA A	GAA GGT ATC AGG GCT GGA ATC
BMF	AGG TAC AGA TTG CCC GAA AG	TGC CAC CAC ACA CGA TTT
BBC3	TGG AGG GTC CTG TAC AAT CT	CAC CTA ATT GGG CTC CAT CTC
BCL2L14	GCC TTG CAG AAA TTC CCA ATC	GCG AAT CTT CCT TCT CCA CTA C
PMAIP1	TGG AAG TCG AGT GTG CTA CT	GTT CCT GAG CAG AAG AGT TTG G
TNFRSF10B	CTG TTC TCT CTC AGG CAT CAT C	GGA AGG ACT TTC TTC CAC AGT AA
TP53	GGA AAT TTG CGT GTG GAG TAT TT	GTT GTA GTG GAT GGT GGT ACA G
TNFSF10	CAG AGA GTA GCA GCT CAC ATA AC	CCT TGA TGA TTC CCA GGA GTT T
GAPDH	GGT GTG AAC CAT GAG AAG TAT GA	GAG TCC TTC CAC GAT ACC AAA G
H3F3A	GCC TAT CTG GTT GGC CTT T	CGT GCT AGC TGG ATG TCT TT
HDAC1	GCT GGC AAA GGC AAG TAT TAT G	CTA GGC TGG AAC ATC TCC ATT AC
CDKN1A	GAG CGA TGG AAC TTC GAC TT	GCT TCC TCT TGG AGA AGA TCA G
TRAF1	AGT CTG TGC AAG AGC ATG AG	GCC ATA CTT GGC AGT GTA GAA
GADD45A	AGA AGA CCG AAA GGA TGG ATA AG	GAT CAG GGT GAA GTG GAT CTG
CASP9	GTC GAA GCC AAC CCT AGA AA	CAC CAA ATC CTC CAG AAC CA
BCL2A1	GTA GAC ACT GCC AGA ACA CTA TT	AAG TCA TCC AGC CAG ATT TAG G
BIRC3	CAA GCC AGT TAC CCT CAT CTA C	CCT CAG TTG CTC TTT CTC TCT C
PML	AAG CCT TCT TCA GCA TCT ACT C	GCT TGT AGC AGG CCA AGA TA
CASP8	GGA GCT GCT CTT CCG AAT TA	CAT GAC CCT GTA GGC AGA AA
CASP2	CCT CAA CTT GCT GCC TAA GA	AGG GTG GTG AGC AAC ATA TC
CASP10	GGA CAG ACA AGG AAC CCA TAA A	TGC AGG ACC ATC TCC ATT TC
GZMB	CCA GCA GTT TAT CCC TGT GAA	CCT CTT GTA GTG TGT GTG AGT G
BCL2L11	CAG ATA TGC GCC CAG AGA TAT G	GTC TTC GGC TGC TTG GTA AT
BAX	TTC TGA CGG CAA CTT CAA CT	CAG CCC ATG ATG GTT CTG AT
CASP3	CTC CAC AGC ACC TGG TTA TT	AAA TTC AAG CTT GTC GGC ATA C
CASP7	CTG ACT TCC TCT TCG CCT ATT C	TCT GCA TGA TTT CCA GGT CTT
JUN	AGA TGG AAA CGA CCT TCT ATG AC	CCG TTG CTG GAC TGG ATT AT

	Forward Primers	Reverse Primers
CXCL8	TTG GCA GCC TTC CTG ATT T	AAA CTT CTC CAC AAC CCT CTG
PLAU	GAG GGC AGC ACT GTG AAA TA	CCG GAT AGA GAT AGT CGG TAG AA
CEBPA	CAT CGA CAT CAG CGC CTA C	GTT CTT GTC CAC CGA CTT CTT
WT1	CGG AGC CCA ATA CAG AAT ACA	GAG CTG GTC TGA ACG AGA AA
NFKBIZ	GGG CTC CCA ACA AAT GAT AGA	GAG GAA GTC TGC ATG GGA TTA G
FLT1	CGT GTG GTC TTA CGG AGT ATT G	GAG AAG GCA GGA GTT GAG TAT G
TFE3	CGG GAT TGT TGC TGA CAT AGA	TCA CTG GAC TTA GGG ATG AGA G
BCL6	CTC AAC AGC CTC AAC CAG AA	CCA CAG ATT TCA CAG GGA TAG G
PDGFA	CGT AGG GAC TGA GGA TTC TTT G	TGG CTT CTT CCT GAC GTA TTC
ZBTB16	CCC TTC AGT CTC CAC TTC ATT T	TTC TCA GCC GCA AAC TAT CC
PPARG	GCC TGC ATC TCC ACC TTA TT	AGC GGG AAG GAC TTT ATG TAT G
GADD45B	GTC GGC CAA GTT GAT GAA TG	GCG TTC CTG AAG AGA GAT GTA G
SIN3A	CTG CTG GAT GGC AAC ATA GA	CTG GCC TTG GCT CTG AAT AA
CEBPB	TTC CTC TCC GAC CTC TTC TC	GCT TGT CCA CGG TCT TCT T
RXRA	CCT CTT TAA CCC TGA CTC CAA G	GCC TCC AGC ATC TCC ATA AG
ZBTB17	GGT GGA CGG TGT TCA CTT TA	CTT CTC CTC TTT GGC TCT CTT G
IGF1R	GCA GAG TGG ATA ACA AGG AGA G	GAG CGA TGA TCA GAT GGA TGA A
LYL1	CAT GAC TGA GAA GGC AGA GAT G	GCT GCT AGG GAA GAT GCT AAA
DUSP6	CAT TGC TTG GCT GGC ATT AG	AGA GAG TCC ACC TGG TAT ACA T
JMJD1C	GGA CGA CAT AGA CAG CCT AAA C	GAC CTG CGT CGT GAT GTA AT
MPO	CCA TGC ACA CCC TCT TAC TT	CAT CAG TTT CCT CGC CAA TTT C
NFKB1	CAC CCT GAC CTT GCC TAT TT	GAA CTC CAG CAC TCT CTT CTT T
NCOR1	CGG CAG AGA CAA GAA CAG ATA G	TGG CAG TCC AAG AGA GAT AGA
PER2	GGA GTT AGA GAT GGT GGA AGA TG	CTC AGA TGA GTC TCG AGG TTT G
HMGA2	AGG AAG CAG CAG CAA GAA	GAC TCT TGT GAG GAT GTC TCT TC
ETV6	ACC AAA GAG GAC TTT CGC TAT C	TTC AAT GGT GGG AGG GTT ATG
RUNX1	CAC TCT GAC CAT CAC TGT CTT C	TGG TTG GAT CTG CCT TGT ATC

	Forward Primers	Reverse Primers
MYC	CTG AGG AGG AAC AAG AAG ATG AG	CTT GGA CGG ACA GGA TGT ATG
FUT8	ACT GGT TCA GCG GAG AAT AAC	CTG GTA CAG CCA AGG GTA AAT
PAX8	CAC TCA CCC TTC GCC ATA AA	CCA TAG GCA TTG CCA GAG TAT
MAX	AAC GTA GGG ACC ACA TCA AAG	GTT GGT GTA GAG GCT GTT GT
RUNX2	CAC TAT CCA GCC ACC TTT ACT T	AGC GTC AAC ACC ATC ATT CT
RARA	GAG CAG CAG TTC TGA AGA GAT AG	TGC TTC GCA GGT CAG TAA TC
CD86	GCC TGA GTG AGC TAG TAG TAT TT	GGT TCT GGG TAA CCG TGT ATA G
AFF1	TCC CAA GCA GAG AAG AGT AGA G	CAA AGG TCA AAG GCG GTA AGA
SLC45A3	CAG GTG TTC CTG CCC AAA TA	CTG GAC AAT GGA GCC CAT AAA
CCNA1	CTC CTC TCC CAG TCT GAA GAT A	GGA AGT TGA CAG CCA GAT ACA
NGFR	GAC AAC CTC ATC CCT GTC TAT T	CCT CAT GGG TAA AGG AGT CTA TG
FLT3	CAA GAA ACG ACA CCG GAT ACT	TTC CAG GTC CAA GAT GGT AAT G
BAK1	ACC CAG AGA TGG TCA CCT TA	AAC AGA ACC ACA CCC AGA AC
ITGB7	CGG TGA CTT TCT GGG TTT CT	CTC CTT CTC AAA GCG ACT GTA T
TLX1	GGC TCC TAC AAC GTG AAC AT	ACC TGT GAA CCT GTC CTT TG
SIX1	TGC CGT CGT TTG GCT TTA	GCT TGT TGG AGG AGG AGT TAT T
EYA1	CTC ACC GTA TCC AGC ACA TTA T	CTA ACC CAT ACA GCA GGA CTT T
ETV7	CTG CTC CTT GAT ACC CGA TAT G	CCA TCT TTC CCG GAG TCT TTA G
MITF	GAG TCA GAC ACC AGC CAT AAA	GAG ACC CGT GGA TGG AAT AAG

Table S5. Fold changes of apoptosis related genes in NB4 cells treated with ZIO-101.

Gene Symbol	Gene Description	Fold Changes (6, 12, 24 hrs)
CASP3	Caspase-3	1.2, 1.9, 1.5
CASP8	Caspase-8	1.1, 1.7, 2.7
CASP9	Caspase-9	1.4, 1.9, 3.4
BAX	Apoptosis regulator BAX	1.2, 1.8, 2.6
BMF	Bcl-2-modifying factor	1.1, 4.3, 24.6
BBC3	Bcl-2-binding component 3	6.7, 7.5, 5.2
BCL2L11	Bcl-2-like protein 11	1.3, 3.0, 2.6

Supplementary Text

To investigate whether the binding of ZIO-101 to cysteine could affect the formation of histone H3.3 dimers through inter-molecule disulfide bonds, histone H3.3 was dialyzed in buffer containing ZIO-101 or DTT and then analyzed by modified SDS-PAGE. As shown in Fig. S10 (ESI[†]), the binding of ZIO-101 to histone H3.3 prevents the dimerization of histone H3.3.

The effect of binding of ZIO-101 to histone H3.3 on the nucleosome structure were studied. The secondary structures of recombinant H3.3 core histone proteins (SKU: 16-8012, EpiCypher) with or without arsenic treatments were examined by circular dichroism spectroscopy. Two characteristic bands at 222 and 208 nm, representing α -helical contents, were observed in histone cores in the absence of ZIO-101 and α -helical contents increased upon ZIO-101 treatment (Fig. S11, ESI[†]), implying that the secondary structure of the nucleosome changed after treatment with ZIO-101.

To further examine whether the secondary structure rearrangement of histone cores owing to the binding of ZIO-101 could affect the stability of nucleosomes, the nucleosome thermal denaturation process was monitored by measuring the absorbance at 260 nm (Fig. S12, ESI[†]). Using nucleosomes containing untreated histone H3.3 as a control, a fusion temperature (T_m) was determined to be 81.6 ± 2.8 °C. A decrease in the DNA melting temperature to 76.3 ± 1.4 °C was observed for nucleosomes consisting of ZIO-101 treated histone H3.3, showing that the nucleosome stability was disrupted. Our combined data clearly demonstrate that binding of ZIO-101 to histone H3.3 facilitates the denaturation of nucleosomes.

References

1. L. Hu, T. Cheng, B. He, L. Li, Y. Wang, Y. Lai, G. Jiang and H. Sun, *Angew. Chem. Int. Ed.*, 2013, **125**, 5016-5020.
2. S. Komatsu, *Methods Mol. Biol.*, 2007, **355**, 73-77.
3. N. Jakubowski, J. Messerschmidt, M. Añorbe, L. Waentig, H. Hayena and P. Roosb, *J. Anal. At. Spectrom.*, 2008, **23**, 1487-1496.
4. L. Zhong, E. Arner and A. Holmgren, *Proc. Natl. Acad. Sci. U S A.*, 2000, **97**, 5854-5859.
5. K. Tatchell and K. Holde, *Biochemistry*, 1977, **16**, 5295-5303.
6. P. Lewis and S. Chiu, *Eur. J. Biochem.*, 1980, **109**, 369-376.
7. J. García-Giménez, G. Òlaso and S. Hake, *Antioxid. Redox Signal.*, 2012, **19**, 1305-1320.
8. S. A. Bustin, V. Benes, J. A. Garson, J. Hellemans, J. Huggett, M. Kubista, *Clin. Chem.*, 2009, **55**, 611-622.
9. Y. Lai, Z. Xu and Y. A., *Environ. Microbiol.*, 2017, **19**, 598-610.
10. J. M. Hearn, I. Romero-Canelónb, A. F. Munro, Y. Fu, P. J. Sadler, *Proc. Natl. Acad. Sci. U S A.*, 2015, **112**, E3800-3805.
11. L. Guan, B. Han, J. Li, Z. Li, F. Huang, Y. Yang and C. Xu, *Ann. Hematol.*, 2009, **88**, 733-742.